Characteristics of an organic photodetector with a conjugated donor and non-fullerene acceptor for indirect X-ray detection

D. Ban, K. Yoo and J. Kang[1]

Department of Electronics and Electrical Engineering, Dankook University,
152 Jukjeon-ro, Suji-gu, Yongin-si, Gyeonggi-do, 16890, Korea

E-mail: jkang@dankook.ac.kr

ABSTRACT: In this study, an organic photodetector with a small band-gap donor, PBDB-T, and a non-fullerene acceptor, ITIC, was investigated as the active element in an indirect imaging system using a scintillator of the detector for indirect X-ray imaging. Compared with the common organic photodetector with a P3HT:$PC_{70}BM$ active layer, higher conversion efficiencies can be expected, because the proposed detector is advantageous for visible-light absorption and carrier transport. The absorption peak of the PBDB-T:ITIC layer was located at 640 nm and was not well-matched with the emission properties of a CsI(Tl) scintillator. Therefore, a ZnSe(Te) scintillator with an emission peak at 620 nm was also tested. Compared with the P3HT:$PC_{70}BM$ detector, the ZnSe(Te)-coupled detector with the PBDB-T:ITIC = 1:1 active layer was 191% higher in collected current density (CCD) and 205% higher in sensitivity. The frequency response was measured with a 520 nm green LED. The detector with the PBDB-T:ITIC layer showed the -3 dB cut-off frequency of 31.5 kHz, which was higher than the cut-off frequency of the P3HT:$PC_{70}BM$ detector.

---

[1]Corresponding author.

Contents

1 Introduction

The application of organic semiconductors has been expanding because of their numerous advantages, such as easy processing, ease of scale-up, light weight, and mechanical flexibility. In addition, the fine extinction property, excellent power-conversion efficiency, and good carrier-transfer ability of organic materials make them suitable for radiation-detector applications. In this respect, organic polymers were reported as materials for radiation detectors in the early 1980s [1], and researchers were fascinated by the possibility of creating new detectors. Organic semiconductor-based X-ray detectors can be divided into two types, the direct type and the indirect type, depending on the detection method. In the indirect-type detectors, X-rays are converted directly into charges in the photoconductor layer. In scintillator-combined indirect detectors, visible photons are generated in the scintillator by incident X-rays, and converted into charges in the organic active layer. In this paper, an indirect-type organic detector with the advantage of relatively high conversion efficiency was studied.

In indirect organic detectors, the conjugate polymer poly(3-hexylthiophene-2,5-diyl) (P3HT) and the fullerene derivatives [6,6]-phenyl-C71-butyric acid methyl ester (PC$_{70}$BM) have been commonly used as donor and acceptor materials to form the active layer. The P3HT has a relatively large band gap, which limits the absorption of visible light. To overcome this problem, other small band-gap donors, such as poly[N-9'-heptadecanyl-2,7-carbazole-alt-5,5-(4',7'-di-2-thienyl-2',1',3'-benzothiadiazole)] (PCDTBT) [2], poly({4,8-bis[(2-ethylhexyl)oxy] benzo[1,2-b:4,5-b′]dithiophene-2,6-diyl}{3-fluoro-2-[(2-ethylhexyl)carbonyl]thieno[3,4-b]thiophenediyl}) (PTB7) [3], poly[[4,8-bis[5-(2-ethylhexyl)-2-thienyl]benzo[1,2-b:4,5-b']dithiophene-2,6-diyl]-2,5-thiophenediyl[5,7-bis(2-ethylhexyl)-4,8-dioxo-4H,8H-benzo[1,2c:4,5-c']dithiophene-1,3-diyl]]) (PBDB-T) and poly[(2,6-(4,8-bis(5-(2-ethylhexylthio)-4-fluorothiophen-2-yl)-benzo[1,2-b:4,5-b′] dithiophene))-alt-(5,5-(1′,3′-di-2-thienyl-5′,7′-bis(2-ethylhexyl)benzo[1′,2′-c:4′,5′-c′]dithiophene -4,8-dione)] (PBDB-T-SF) [4] have been tested as alternatives. The PC$_{70}$BM with a fullerene-based bucky-ball structure has the drawbacks of high synthetic cost, low extinction coefficient, and poor morphological stability. Therefore, non-fullerene acceptors with an expanded net structure have

recently been studied. The 5,5′-[(9,9-Dioctyl-9H-fluorene-2,7-diyl)bis(2,1,3-benzothiadiazole-7,4-diylmethylidyne)]bis[3-ethyl-2-thioxo-4-thiazolidinone] (FBR) [5], rhodanine-benzothiadiazole-coupled indacenodithiophene alkylated using linear n-octyl (O-IDTBR) [6] and 2,2′-((2Z,2′Z)-(((4,4,9-tris(4-hexylphenyl)-9-(4-pentylphenyl)-4,9-dihydro-s-indaceno[1,2-b:5,6-bdithiophene-2,7-diyl)bis(4-((2-ethylhexyl)oxy)thiophene-5,2-diyl))bis(methanylylidene))bis(5,6-dichloro-3-oxo-2,3-dihydro-1H-indene-2,1-diylidene))dimalononitrile (IEICO-4Cl) [7] were applied as alternative non-fullerene acceptors.

In this study, we selected the previously studied PBDB-T as a donor, and the $PC_{70}BM$ acceptor was substituted for 2,2′-[[6,6,12,12-Tetrakis(4-hexylphenyl)-6,12-dihydrodithieno[2,3-d:2′,3′-d′]-s-indaceno[1,2-b:5,6-b′]dithiophene-2,8-diyl]bis[methylidyne(3-oxo-1H-indene-2,1(3H)-diylidene)]]bispropanedinitrile (ITIC) to improve the performance of the organic detector. As is shown by figure 1(a), the ITIC works better than the $PC_{70}BM$ because of the two 2-(3-oxo-2,3-dihydroinden-1-ylidene)malononitrile (INCN) groups with strong electron-suction properties and its push-pull structure improving the carrier transport and light absorption properties [8]. ITIC has a smaller ΔLUMO and ΔHOMO with PBDB-T than does $PC_{70}BM$, where ΔLUMO and ΔHOMO are the differences between the lowest unoccupied molecular orbital (LUMO) and the highest occupied molecular orbital (HOMO) levels of each donor and acceptor. If these values are small, they reduce energy loss during the separation of excitons inside the active layer [9]. In addition, ITIC is a non-fullerene acceptor with excellent mechanical flexibility, so it can be applied to flexible detectors.

Figure 1(b) shows the absorption spectrum of each material constituting the active layer. The PBDB-T and ITIC selected in this study show relatively high absorbance compared to P3HT and $PC_{70}BM$, which are commonly used. In order to improve the sensitivity of the indirect-type detector, the match between the emission wavelength of the combined scintillator and the absorption spectrum of the detector is important. Considering the absorption spectra of PBDB-T and ITIC shifted toward longer wavelength region, we evaluated the detector characteristics using a ZnSe(Te) scintillator with a peak emission of 640 nm along with a common CsI(Tl) scintillator with a peak emission of 550 nm. To find the optimum process conditions of the detector having the PBDB-T:ITIC active layer, we examined the mixing ratio of the PBDB-T:ITIC films and then the thickness of the active layer while adjusting the spin-coating conditions. In addition to detection sensitivity, the frequency response is also an important parameter for imaging application. In recent years, there is a growing demand for X-ray imaging systems that feature high resolution and low dose rates. In addition to detection sensitivity, the frequency response is also an important parameter for imaging application. Using a flashing green LED, the frequency response of the scintillator-decoupled detector was evaluated and compared it with that of the silicon photodiode.

2 Experimental preparation

2.1 Device preparation

Figure 2(a) shows the structure of the indirect-type X-ray detector with an organic active layer. The procedure for fabricating the detector is as follows. The indium-tin-oxide (ITO) anodes on glass substrates were patterned, and then the ITO-patterned substrates were cleaned sequentially
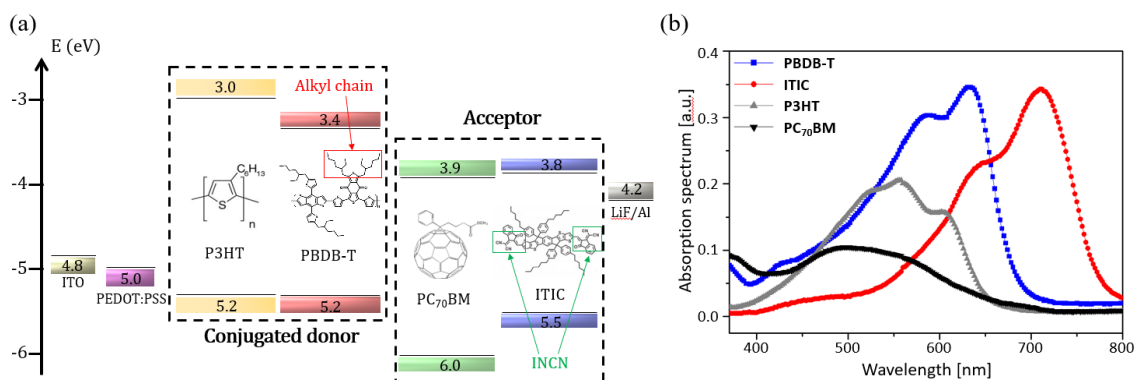
Figure 1. (a) Energy band diagram of the proposed detector and (b) absorption spectra of various organic materials.

with acetone, methanol, and isopropyl alcohol. The cleaned substrates were dried for 10 min in a vacuum oven at 100°C. Poly(3,4-ethylenedioxythiophene):poly(styrenesulfonate) (PEDOT:PSS) solution working as the hole-transport layer (HTL) was spin-coated at 3,000 rpm, and then 50 wt% of N,N-dimethylmethanamide (DMF) solvent was added to improve the conductivity of the HTL. The DMF-treated HTL was annealed at 150°C for 10 min. The PBDB-T and ITIC materials forming the active layer were dissolved in a chlorobenzene solvent at mixing ratios of 2:1, 1:1, 1:2, and 1:3, and stirred at 90°C for 3 hrs. The PBDB-T:ITIC solutions were spin-coated on the PEDOT:PSS HTL with different spin-rates of 1500, 2000, 2500, 3000, and 3500 rpm, and baked at 150°C for 10 min. The cathode, consisting of LiF/Al, was deposited by thermal evaporation, and finally the glass cover was attached to protect the fabricated detector from oxygen and moisture. In the presence of oxygen and moisture, the detector degradation occurs due to chemical interactions with oxidizing agent. For the comparison, we also fabricated the reference detector with a 1:1 mixed P3HT:PC$_{70}$BM active layer (the common mixing ratio used for organic detectors [10]). The image of the fabricated detector is shown in figure 2(b). There were four pixels in one detector, and the effective area of each cell was 4 mm^2.
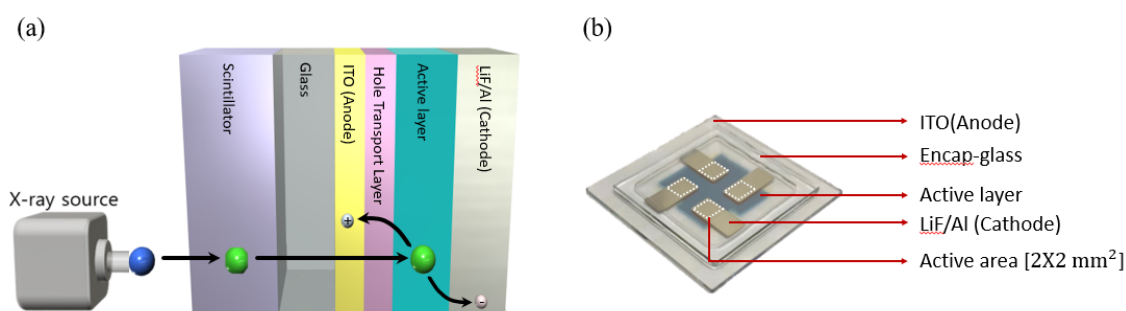

Figure 2. (a) Schematic diagram of the indirect-type organic X-ray detector and (b) real image of the fabricated detector.

2.2 Experimental set-up

An experiment apparatus for evaluating the performance of the detector is shown in figure 3. Before evaluating its performance as an X-ray detector, we first evaluated the characteristics of the scintillator-isolated photodetector by using a solar simulator (San Ei Elec. XES 40S2-CE) to investigate the intrinsic characteristics of the photodetector. Since the indirect-type detector is composed of a scintillator and photodetector, it is necessary to investigate the performance of the photodetector individually. While illuminating a Xe lamp filtered with AM 1.5G in the solar simulator, the generated carriers were collected with an electrometer (Keithley 2400) at a bias from -1.0 V to 1.0 V. The distance between the filtered lamp and the detector is 25 cm, at which point the light intensity is 100 mW/cm^2. From the current density-voltage (J-V) characteristics, we calculated the evaluation parameters, such as the power-conversion efficiency (PCE) and short-circuit current density (J_{SC}) of the photodetector [11]. An X-ray generator (AJEX 2000H) was used to examine the properties of the scintillator-coupled detector. The operating condition was fixed at 80 kV$_p$ and 63 mAs, and the exposure time was 1.57 s for all experiments. The distance between the X-ray generator and the detector was fixed at 30 cm, and the exposed dose was measured with an ion chamber (Capintec CII50) at the same position as the detector. The absorbed dose was converted from the exposure, which was measured using the ion chamber. Under the conditions mentioned above, the absorbed dose was 3.44 mGy. We extracted radiation parameters, such as the collected current density (CCD) during X-ray exposure, dark current density (DCD) during X-ray off-condition. The sensitivity was calculated using the following equation. The difference in collected current during the X-ray on and off conditions was divided by the product of exposure area (4 mm^2) and absorbed dose.

$$\text{Sensitivity} \left[\frac{\text{mA}}{\text{Gy} \cdot \text{cm}^2} \right] = \frac{\text{Currents during X–ray ON} - \text{Currents during X–ray OFF}}{\text{Absorbed Dose} \times \text{Exposed Detection Area}}$$
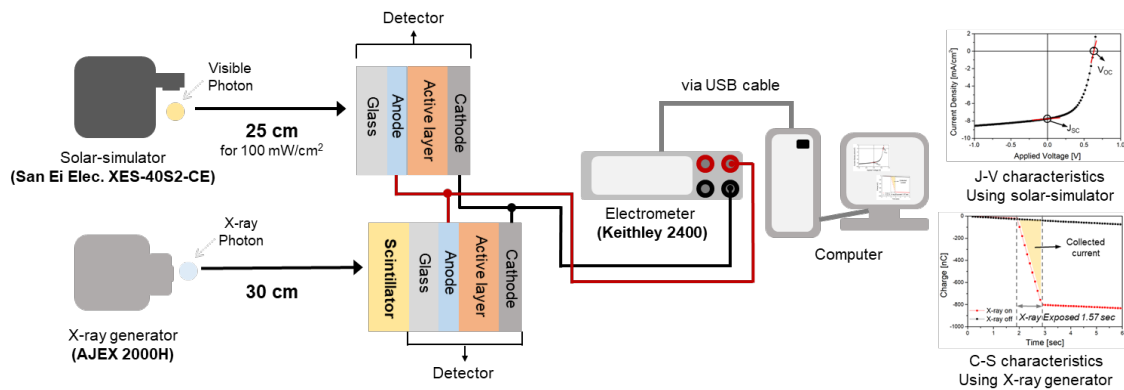

Figure 3. Experimental apparatus for measuring the properties (J_{SC} and PCE) of the scintillator-isolated detector properties and radiation properties (CCD, DCD, and sensitivity) of the scintillator-coupled detector.

3 Result and discussion

We investigated the properties of the photodetector, which depend on the mixing ratio and thickness of the PBDB-T:ITIC active layer, under artificial solar irradiation. Figure 4(a) shows the J-V characteristics of five different samples, four with different mixing ratios of PBDB-T:ITIC and a reference sample with a P3HT:PC$_{70}$BM active layer. We calculated the highest J$_{SC}$ of 17.15 mA/cm^2 and highest PCE of 7.40% at the photodetector with the PBDB-T:ITIC = 1:1 mixed layer. Compared to the reference detector with the P3HT:PC$_{70}$BM active layer, the PCE improved 285%. In figure 4(b), after fixing the mixing ratio to PBDB-T:ITIC = 1:1, the characteristics of the photodetector were measured by altering the thickness of the active layer while changing the spin-coating conditions. For the detector with the P3HT:PC$_{70}$BM, the optimal thickness of the active layer was about 120 nm. The optimal thickness of the PBDB-T:ITIC active layer was investigated by changing the spin-coating condition from 1,500 rpm to 3,000 rpm. As the spin-rate was increased, the thickness of the active layer was decreased, and the percolation path for the collecting carrier was well formed. However, the active layer became so thin that the percolation path was not properly formed [12]. The highest J$_{SC}$ of 18.04 mA/cm^2 and highest PCE of 8.65% were calculated for the PBDB-T:ITIC photodetector with a spin-rate of 2,500 rpm and thickness of about 104 nm. By our finding the optimal active-layer thickness, the PCE increased by 330% compared with the PCE of the reference detector.
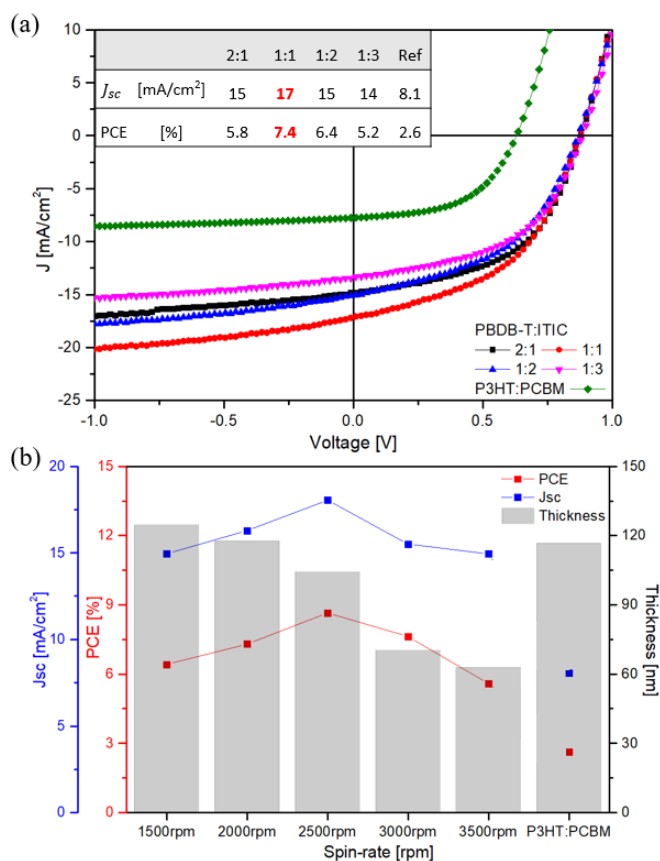

Figure 4. (a) J-V characteristic of the photodetectors depending on the PBDB-T:ITIC mixing ratios and (b) J$_{SC}$, PCE, and thickness of the active layer depending on the spin-coating conditions. detector.

Figure 5 shows the absorption spectra of the 1:1 mixing ratio of P3HT:PC$_{70}$BM and different mixing ratios of PBDB-T:ITIC measured with a UV/vis spectrometer (Optizen 2120UV). The emission spectra of the CsI(Tl) and ZnSe(Te) scintillators are also shown. The CsI(Tl) scintillator, which is a commonly used scintillator because of its high light yield, has a emission peak at 550 nm, and its emission spectrum is well-matched with the absorption spectrum of the P3HT:PC$_{70}$BM active layer. The absorbance of the PBDB-T:ITIC active layer was relatively higher in the visible region than that of the P3HT:PC$_{70}$BM. However, the absorption peak was located at 640 nm and was not well matched with the emission property of the CsI(Tl). For this reason, a ZnSe(Te) scintillator with an emission peak at 620 nm was also tested. The ZnSe(Te) scintillator has a higher density than the CsI(Tl) scintillator and has the advantage of being more stable and a faster decay time. The ZnSe(Te) scintillator shows a 25% lower light yield than CsI(Tl), but considering the matching with the absorption spectrum of the PBDB-T:ITIC, more visible photons can be generated from the ZnSe(Te) scintillator. The highest absorbance was measured at the condition of PBDB-T:ITIC = 1:1 mixed layer. As shown in figure 4(a), the highest J$_{SC}$ and PCE were obtained in the photodetector with the same active layer.
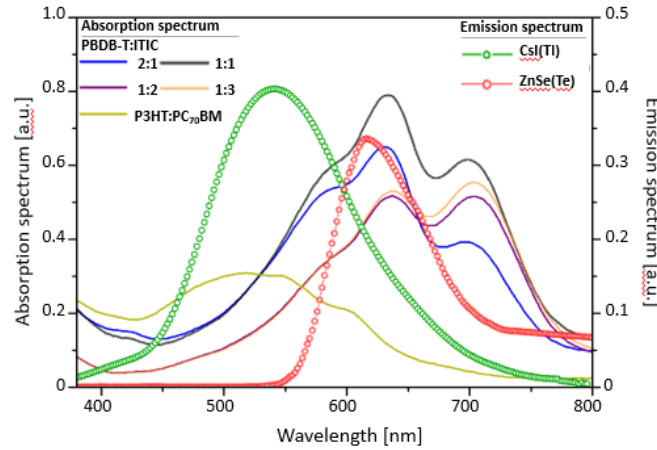

Figure 5. The absorption spectra of the P3HT:PC$_{70}$BM and PBDB-T:ITIC thin films and emission sperctra of the CsI(Tl) and ZnSe(Te) scintillators.

We measured the characteristics of the scintillator-coupled detectors during X-ray exposure. The operation conditions of the X-ray source are described in section 2.2. Two scintillators, CsI(Tl) and ZnSe(Te), were applied to the detectors, such as the reference detector with the P3HT:PC$_{70}$BM layer and the detectors with different mixing ratios of the PBDB-T:ITIC layer. The radiation parameters, such as CCD and sensitivity, were calculated from the J-V characteristics of the detectors and are depicted in figure 6(a). The ZnSe(Te) scintillator combined detector with the PBDB-T:ITIC = 1:1 active layer showed the highest CCD of 7.1 μA/cm^2 and highest sensitivity of 1.91 mA/Gy·cm^2. The same detector combined with the CsI(Tl) scintillator showed a lower CCD of 4.35 μA/cm^2 and lower sensitivity of 1.12 mA/Gy·cm^2, mainly because of the absorbance characteristic of the PBDB-T:ITIC thin film depicted in figure 5. The DCD value of the detector with the PBDB-T:ITIC = 1:1 active layer was 0.53 μA/cm^2. The CsI(Tl) scintillator-coupled reference detector with the P3HT:PC$_{70}$BM layer showed a CCD of 3.71 μA/cm^2 and sensitivity of

0.93 mA/Gy·cm^2. The absorbance property of the P3HT:PC$_{70}$BM film was well-matched with the emission property of the CsI(Tl) scintillator. Therefore, the sensitivity with CsI(Tl) was higher than the sensitivity obtained with ZnSe(Te). Compared with the reference detector combined with CsI(Tl), the ZnSe(Te)-coupled detector with the PBDB-T:ITIC = 1:1 layer was 191% higher in CCD and 205% higher in sensitivity, and the tendency was similar to the previous results collected under artificial solar irradiation. In figure 6(b), the surface roughness (R$_q$) changed by the PBDB-T:ITIC mixing ratio is shown and the roughness was measured by atomic force microscope (AFM). As R$_q$ decreased, the series resistance of the detector tended to decrease. The R$_q$ of the PBDB-T:ITIC = 1:1 ratio film was the lowest value, of 1.60 nm, and the series resistance of the detector with the same active layer was the lowest value, of 391.8 Ω. The PBDB-T:ITIC = 1:1 active layer exhibited the highest absorbance needed to generate the carriers and also showed the lowest roughness and resistance needed to transport the carriers.
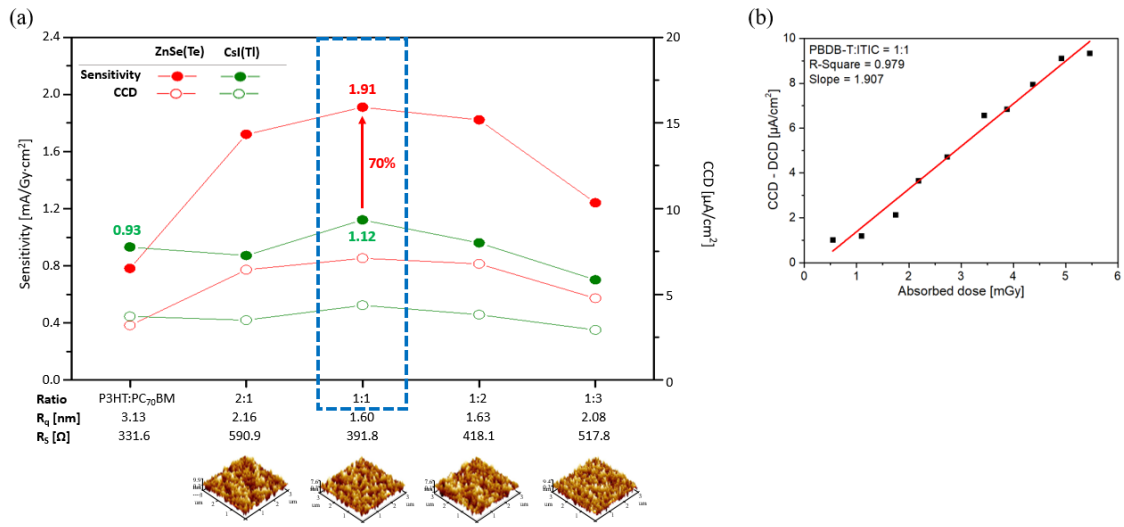

Figure 6. (a) Radiation parameters of the combined CsI(Tl), ZnSe(Te) scintillators and AFM images according to the PBDB-T:ITIC mixing ratios and (b) collected current density during the X-ray on and off conditions of the detector with PBDB-T:ITIC = 1:1 active layer and ZnSe(Te) scintillator depending on the absorbed dose.

Amongst the characteristics of the detector, the frequency response is one of the important parameters, especially for the image detector applications. A detector with a fast frequency response is advantageous for building clear images in a short time. The experimental set-up to measure the frequency response is shown in figure 7(a). The intensity of a green LED with an emission of 540 nm was fixed at 60 μW/cm^2 and a green-pulsed light with a frequency range from 2 Hz to 100 kHz and 50% duty cycle was radiated to the scintillator-separated detector. At the bottom of figure 7(a), the signal response of the organic detector with the PBDB-T:ITIC = 1:1 layer and silicon detector (Hamamatsu S3590-08) is depicted with square light pulses at 2 Hz and 1 kHz frequencies. All signals were measured with an oscilloscope (LeCroy 104Xi). The amplitude difference at the lowest frequency (in this case, 2 Hz) was defined as U$_0$ and the amplitude difference at different frequencies was defined as U. From the U/U$_0$ ratio, the amplitude bode plot was extracted as shown in figure 7(b). The cut-off frequency is defined as the frequency at which the amplitude of signal

falls to $1/\sqrt{2}$ from the signal at low frequency. The cut-off frequency corresponds to the -3 dB green line in the amplitude bode plot. The detector with the P3HT:PC$_{70}$BM layer showed a cut-off frequency of 27.5 kHz, and the detector with the PBDB-T:ITIC layer showed a cut-off frequency of 31.5 kHz, which was smaller than that of the silicon photodetector (53 kHz) with the same experimental set-up. Since the cut-off frequency of the proposed detector is more than 60% of the cut-off frequency of the silicon photodetector, it can be seen that there is no problem when driving the detector [13].
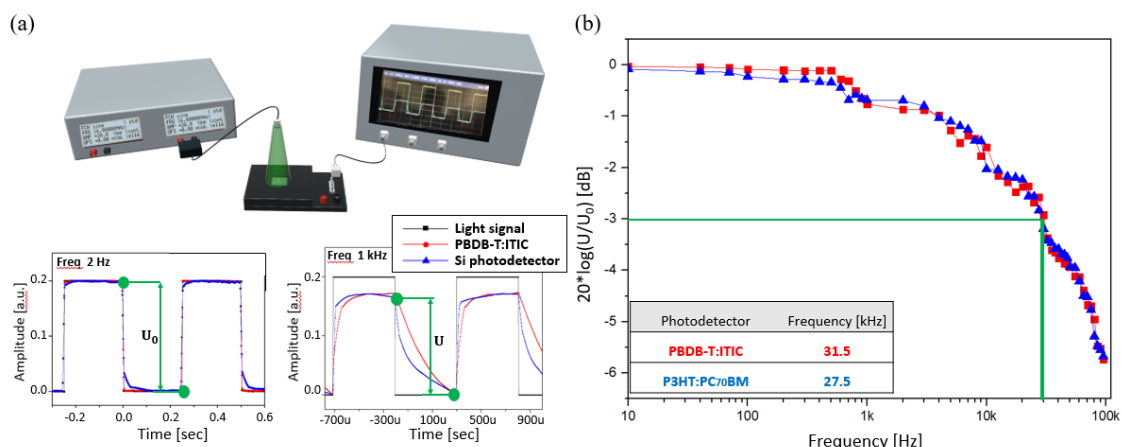

Figure 7. (a) Experimental set-up for measuring frequency response and (b) extracted amplitude bode diagram.

4 Conclusion

In this study, we investigated an indirect-type organic X-ray detector made with the small band-gap donor PBDB-T and the non-fullerene acceptor ITIC. Compared with the common organic detector with an P3HT:PC$_{70}$BM active layer, a higher conversion efficiency can be expected because the proposed detector is advantageous for visible-light absorption and carrier transport. The properties of the scintillator-decoupled detector, which vary with the mixing ratio and thickness of the PBDB-T:ITIC active layer, were investigated under artificial solar irradiation. The highest J$_{SC}$ of 18.04 mA/cm^2 and highest PCE of 8.65% were calculated for the PBDB-T:ITIC = 1:1 detector with a spin-rate of 2,500 rpm and thickness of about 104 nm. The PCE increased by 330% compared with the PCE of the P3HT:PC$_{70}$BM detector. The characteristics of the scintillator-coupled detector were measured during X-ray exposure. The absorption peak of the PBDB-T:ITIC film was located at 640 nm and was not well matched with the emission properties of CsI(Tl). Therefore, a ZnSe(Te) scintillator with an emission peak at 620 nm was also tested. Compared with the P3HT:PC$_{70}$BM detector, the ZnSe(Te)-coupled detector with the PBDB-T:ITIC = 1:1 layer was 191% higher in CCD and 205% higher in sensitivity. The frequency response was measured with a 520 nm green LED. The detector with the PBDB-T:ITIC layer showed a cut-off frequency of 31.5 kHz, which was about 60% of the cut-off frequency of the silicon photodetector.

Acknowledgments

References

[1] K. Yoshino, S. Hayashi, G. Ishii and Y. Inuishi, *Electrical transport in electron beam irradiated polyacetylene*, *Solid State Commun.* **5** (1983) 405.

[2] H. Seon, D. Ban and J. Kang, *A study on the characteristics of indirect-type organic detector using p-type polycarbazole copolymer for X-ray imaging*, 2018 *JINST* **13** C01031.

[3] M. Zhou et al., *Enhancement of power conversion efficiency of PTB7:PCBM-based solar cells by gate bias*, *Org. Electron.* **32** (2016) 34.

[4] W. Zhao et al., *Molecular Optimization Enables over 13% Efficiency in Organic Solar Cells*, *J. Am. Chem. Soc.* **139** (2017) 7148.

[5] S. Holliday et al., *A Rhodanine Flanked Nonfullerene Acceptor for Solution-Processed Organic Photovoltaics*, *J. Am. Chem. Soc.* **137** (2015) 898.

[6] J. Lee and J. Kang, *Characteristics of a Flexible Radiation Detector Fabricated with Non-Fullerene Acceptor for an Indirect-type X-ray Imaging*, 2019 *JINST* **14** C03008.

[7] Y. Cui et al., *Efficient Semitransparent Organic Solar Cells with Tunable Color enabled by an Ultralow-Bandgap Nonfullerene Acceptor*, *Adv. Mater.* **29** (2017) 43.

[8] Z. Kang et al., *Push-Pull Type Non-Fullerene Acceptors for Polymer Solar Cells: Effect of the Donor Core*, *ACS Appl. Mater. Interf.* **9** (2017) 24771.

[9] S.M. Menke, N.A. Ran, G.C. Bazan and R.H. Friend, *Understanding Energy Loss in Organic Solar Cells: Toward a New Efficiency Regime*, *Joule* **2** (2018) 25.

[10] S. Kim, B. Kim and J. Kang, *Characteristics of an Indirect-Type X-ray Detector Fabricated with Organic Semiconductor Materials*, *Nanosci. Nanotechnol.* **7** (2015) 989.

[11] J. Lee, H. Seon and J. Kang, *Comparative Studies Between Photovoltaic and Radiation Parameters in Indirect-Type Organic X-ray Detector with a P3HT:PCBM Active Layer*, *Nanosci. Nanotechnol. Lett.* **9** (2017) 1159.

[12] H. Seon, B. Kim and J. Kang, *Characteristic of an Organic Photodetector Fabricated With P3HT:ICBA Blending Materials for Indirect X-Ray Detection*, *IEEE Trans. Nucl. Sci.* **64** (2017) 1739.

[13] F. Arca et al., *Interface Trap States in Organic Photodiodes*, *Sci. Rep.* **3** (2013) 1324.